Journal of Thermal Analysis, Vol. 25 (1982) 409–422

ADAPTION OF THERMAL ANALYSIS FOR THE STUDY OF WATER VAPOUR ADSORPTION ISOTHERMS

Z. JUHÁSZ

Department of Building Materials, Technical University, 1521 Budapest, Hungary

(Received February 12, 1982)

Water vapour adsorption processes and equilibria on adsorbents with polar surfaces can be well tested with an adsorption method combined with thermal analysis. The first step involves the comparison of isothermal desorption-adsorption curves and thermal curves; in the second step different equilibrium points of the adsorption isotherms are tested by means of thermal analysis.

Some examples of building materials are presented to demonstrate the possibilities of the method. The types of adsorption isotherms for the samples were formally equal in all examples; only the complex method presented was able to reveal that formation of the equilibiria was induced by essentially different processes. Such processes are: physical adsorption depending on the structure of the adsorbent and the activity of the external active centres, chemisorption, chemical reaction in the solid/vapour system and chemical reaction in the water phase condensed in the capillaries.

Water vapour adsorption equilibria on silicates and inorganic building materials are examined from both practical and theoretical aspects. The practical (technical) character of the examinations is determined by the fact that the production and application of these materials often involves their contact with water in some form; hence, the mode of this contact and the properties of the water-containing systems control the production technology and application possibilities. The theoretical investigations have the aim of obtaining more information about the structure of materials, exploiting the fact that the small dipolar water molecules are strongly bound on polar surfaces and may be adsorbed even on internal surfaces that can not be reached by large molecules of other adsorbates.

Water vapour adsorption is generally studied with isothermal and anisothermal methods. The isothermal-static method involves the experimental determination of water vapour adsorption isotherms with any of the methods generally used in adsorption studies [1]. Thermoanalytical instruments [2] (e.g. a derivatograph [3]) are employed in the anisothermal-dynamic method.

In practice difficulties arise in the evaluation of the experimental data in both methods. Accordingly mainly for the correct interpretation of adsorption isotherms, additional examinations (e.g. X-ray, infrared, magnetochemical, thermal, etc.) are often used [4–16].

It is evident that dynamic methods should be used to complement each other. This study will present the possibilities and methods of such complex examination.

Some problems in evaluating water vapour adsorption isotherms

Most of the water vapour adsorption isotherms of the investigated materials (natural and artificial silicates, carbonates, oxides and sulphates of alkaline earth metals, etc.) are curves with inflexion points (Fig. 1) that belong to type II in the BDDT classification [17]. In the range of low vapour pressure to the left of the inflexion point water molecules are generally bound to the adsorbent by adsorption, while to the right of it they are bound by capillary condensation. Throughout the isotherms the vapour pressure above materials with different water contents is lower than the partial vapour pressure above a pure water surface, but it can also be said that in the whole range of the isotherms water molecules are bound more strongly to adsorbents than to the free water surface. This allows the expression of adsorption equilibria by means of three curves:

1. The adsorption isotherm (vapour pressure) curve (Fig. 1a) embodying the relationship between the relative water vapour pressure (humidity, p_r) and the water content in equilibrium (water content, w).

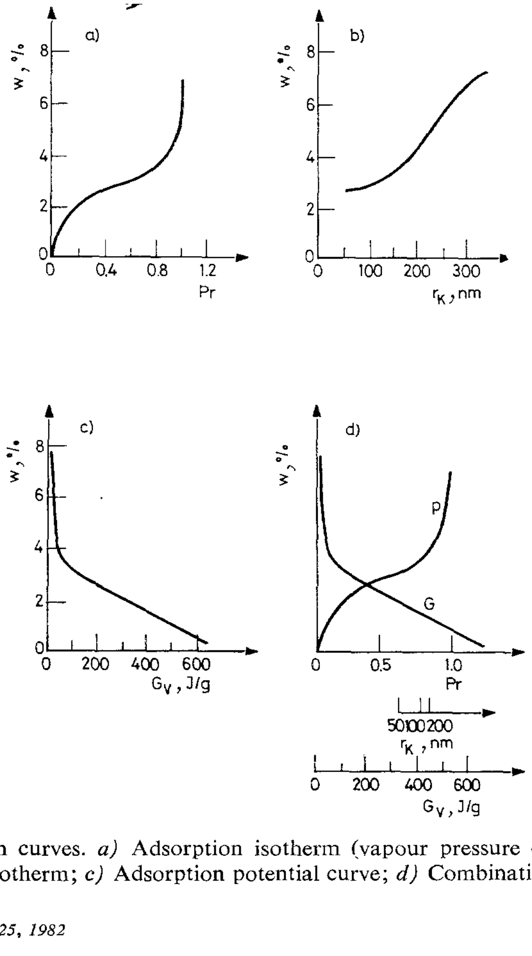

Fig. 1. Adsorption curves. *a)* Adsorption isotherm (vapour pressure curve); *b)* Capillary condensation isotherm; *c)* Adsorption potential curve; *d)* Combination of curves *a*—*c*

2. The capillary condensation isotherm curve (Fig. 1b) embodying the relationship between the capillary radius (r_k) and the water content (w).

3. The adsorption potential curve (Fig. 1c) embodying the relationship between the adsorption potential (G_v) and the water content (w)

The three isotherms can be combined as in Fig. 1d.

The water vapour adsorption isotherm is essentially a curve that presents the relative water vapour pressures of adsorbents with different water contents at the experimental (constant) temperature. The relative vapour pressure is:

$$p_r = \frac{p}{p_t}$$

where p_t is the water vapour pressure at saturation.

To express water vapour adsorption isotherms mathematically, as for all adsorption isotherms, several equations based on various adsorption models [18] are available; these differ formally from one another and the resulting conclusions also often differ.

The most widely-used adsorption equation is the Brunauer–Emmett–Teller (BET) equation [19].

In the evaluation of adsorption isotherms, the problem often arises of how the adsorption models adopted to derive the BET and other equations reflect the actual adsorption processes [20], especially in cases where there are adsorption centres with distinct activities on the surface, chemisorption processes may occur or the sample is a mixture of components (phases) with different adsorption activities etc. The relationship between the water content and the Kelvin radius (r_K) is demonstrated by *capillary condensation isotherms*. The Kelvin radius is:

$$r_K = -\frac{2\gamma V \cos\vartheta}{RT \ln p_r}$$

where γ = surface tension of water, ϑ = wet angle, V = molecular volume of water, T = temperature, and R = gas constant. r_K is not an actual, but an equivalent capillary radius. The Kelvin equation is valid only for capillaries whose diameter is a multiple of that of the water molecule.

Certain circumstances disturb the evaluation of experimental isotherms of silicates and building materials:

(a) Change of size distribution of pore systems in time if the condensed water dissolves the adsorbent or induces chemical reactions in it;

(b) As a consequence of partial dissolution of the adsorbent, the vapour pressure, surface tension and wettability of the water condensed in the capillaries change.

(c) As a result of chemical reactions between materials dissolving in the condensed water, the vapour pressure curves change.

(d) A hysteresis loop occurs in the adsorption-desorption phase, mainly for the smallest Kelvin capillaries.

The *adsorption potential* of Polányi [21] is:

$$G_v = -\frac{RT}{M}\ln p_r.$$

Dubinyin [22] derived approximate equations for the two types of Polányi's "characteristic isotherms", but these were not applicable to our systems.

Principles of the present method

(a) The adsorption properties of the sample can be inferred from the adsorption isotherms (vapour pressure curve) at 20°. The adsorption properties include here the specific surface (S_w), the specific mean adsorption energy of water (E_w), and the specific capillarity (K_w).

(b) It must be ensured that during the preparatory process the adsorption properties of the sample undergo as little change as possible; preliminary drying and overgrinding are to be avoided.

(c) Some points of the adsorption isotherms (i.e. the equilibria relating to different water contents) must be controlled with thermoanalytical methods.

(d) The examination is made in two parts: In the first, the thermal curves and the adsorption isotherm are determined in parallel. For the latter any adsorption instrument [1] can in principle be applied. The two curves are jointly. In the second, samples with different adsorption equilibria are controlled thermoanalytically.

The overall examination may well be performed with the "desiccator method" (see below).

Experimental

Preparation of the sample

The wet sample must be dried in such a way as to avoid irreversible morphological and surface structure changes [23, 24]. Drying in the open air is suggested, or not in excess of 50°. Since grinding may cause mechanochemical changes in the structure [25], the sample is pulverized below 60 μm gradually combined with sifting.

To equilibrate the water content, the pulverized sample is kept in a closed vessel for some days.

Methods

Adsorption

The classic desiccator method [26] is as follows:

2 g samples are weighed in jars of the same size, which are then put into well-closing desiccators with atmospheres of different relative humidities obtained with

salt or sulphuric acid solutions of different concentrations. At least 10–12 desiccators are used in the range $p_r = 0.05-0.99$. In desiccators where the humidity is less than in the laboratory air, desorption of the water occurs; at higher humidities, adsorption of water results. After the attainment of equilibrium, thermal analysis is started immediately.

Thermal analysis

Conditions of thermal analysis: weight of sample: 750 mg, heating rate: 10°/min, atmosphere: air, static, reference material: α-Al_2O_3.

Sometimes, before heating is started a disturbed equilibrium may be restored by passing an atmosphere in which the humidity is equal to the equilibrium humidity through the air space in the oven.

Evaluation of the adsorption isotherms

If the mass of sample measured into the jar is m_0 and the change in mass after attainment of equilibrium is $\Delta m'$, the percentage mass change is:

$$\Delta m = \frac{\Delta m'}{m_0} 100 \ (\%)$$

First the primary potential curve, i.e. the Δm vs. G_v curve, is constructed (Fig. 2a). It is proposed that the Δm axis should be drawn at

$$G_v^0 = -\frac{RT}{M} \ln 0.01$$

where the value of G_v^0 is ≈ 623 J/g at 20°.

Over a broad G_v range, the potential plot is linear, and in this section one may speak of equipotential adsorption. By graphical extrapolation of the straight line, the $\Delta^\circ m$ value relating to the G_v^0 may be obtained. This value is considered the maximum water quantity that can be removed by isothermal desorption at about 20°. Thus the water content relating to any p_r value is:

$$w = \frac{\Delta m - \Delta^\circ m}{100 + \Delta^\circ m} \cdot 100 \ (\%) .$$

From the primary adsorption curve the mass change Δm_t relating to $G_{vt} = -\frac{RT}{M} \ln 0.94$ (~ 10 J/g) can be read off directly.

Then the adsorption isotherm (vapour pressure curve) (p_r vs. w) (Fig. 2) can be constructed and from it the monomolecular saturation (w_m) is obtained, while the specific surface (S_w) is calculated via the graphical method presented in Fig. 2.

The specific mean adsorption energy can also be obtained via the graphical method, as follows:

$$E_w = \frac{\int_{\Delta^\circ m}^{\Delta m_t} G_v \mathrm{d}(\Delta m)}{\Delta m_t - \Delta^\circ m}\ (\mathrm{J/g})$$

E_w is proportional to the section located above the straight line $\Delta^\circ m$ = const. and below the dotted potential curve in Fig. 2.

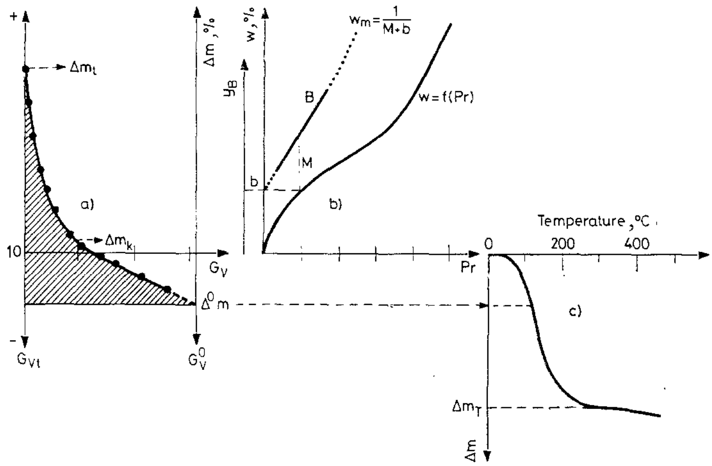

Fig. 2. Scheme of graphical presentation of experimental data. *a)* Primary potential curve; *b)* Adsorption isotherm (vapour pressure curve) and BET equation in the form $y_B = \frac{p}{w(p - p_t)}$ *c)* TG curve combined with potential curve

Finally, the point denoting the limit of the equipotential adsorption stage in the potential curve is established. Here the curve sweeps towards the G_v axis or rises steeply at the critical content:

$$w_k = \frac{\Delta m_k - \Delta^\circ m}{100 + \Delta^\circ m} \cdot 100\%$$

The specific capillarity is

$$K_w = \frac{w_t - w_k}{100 \cdot \varrho_v}\ (\mathrm{ml/g})$$

where ϱ_v is the density of water (ml/g) at the experimental temperature.

It should be noted that $w_k \geq w_m$. If $w_k = w_m$, the increase of the monomolecular layer is immediately followed by capillary condensation. If $w_k > w_m$, polymolecular adsorption may be presumed or perhaps the presence of adsorption centres with different activities. If the adsorption potential curve displays a break-point, with an inclination toward the horizontal, this generally indicates a lack of smaller pores [18].

Comparison of the adsorption isotherm with the TG curve

The evaluation is facilitated if the thermoanalytical curve is combined with the adsorption isotherm and the common axis is the mass loss (Δm) in Fig. 2. The $\Delta^\circ m$ value is projected on to the TG curve. If the whole TG step of the first endothermic reaction is denoted by Δm_T, the strongly adsorbed, the chemisorbed and perhaps the crystal and structural water (gel water) is:

$$w_g = \frac{\Delta m_T - \Delta^\circ m}{100 + \Delta^\circ m} \cdot 100 .$$

The value of w_g has a negative sign in this case.

Some examples of the practical application of the combined method

Some examples will be presented where the types of the water vapour adsorption isotherms of the materials are the same (i.e. BDDT type II), but formation of the adsorption and the water vapour adsorption equilibrium results from essentially different processes.

Water vapour equilibria of SiO_2-H_2O *systems*

Compact granular quartz and silica gel consisting of porous grains are two different types of adsorbents. This difference is reflected in our results.

Experiment. Air-dried and fine-grained samples of quartz (SiO_2) and of silica gel ($SiO_2 \cdot n\,H_2O$) were tested by the above complex method. The second part of the investigation was omitted here because, in our judgement, there was no need for it.

Experimental results (Figs 3 and 4)

The difference between the silicate structures of the two adsorbents is reflected by the DTA curves (the 575° endothermic maximum observed for quartz is totally missing from the silica gel curve). There are also differences in the total dehydration processes of the two materials, the specific surfaces, the specific adsorption energies and the specific capillarities.

In accordance with literature data [16], both materials contain surface OH groups that can be eliminated only at higher temperature. The density of these, the surface hydration degree, is:

$$\alpha_{OH} = \frac{w_g \cdot 10^4}{18 \cdot S_w} (\mu\text{mol/m}^2) .$$

For quartz $\alpha_{OH} = 2.7\ \mu\text{mol/m}^2$, while for silica gel $\alpha_{OH} = 12.0\ \mu\text{mol/m}^2$, which points to different structures.

While quartz powder has a small specific surface and its particles hardly include fine pores, silica gel is characterized by a very large specific surface, with numerous and very fine pores. Both materials have high specific adsorption energies, but tha

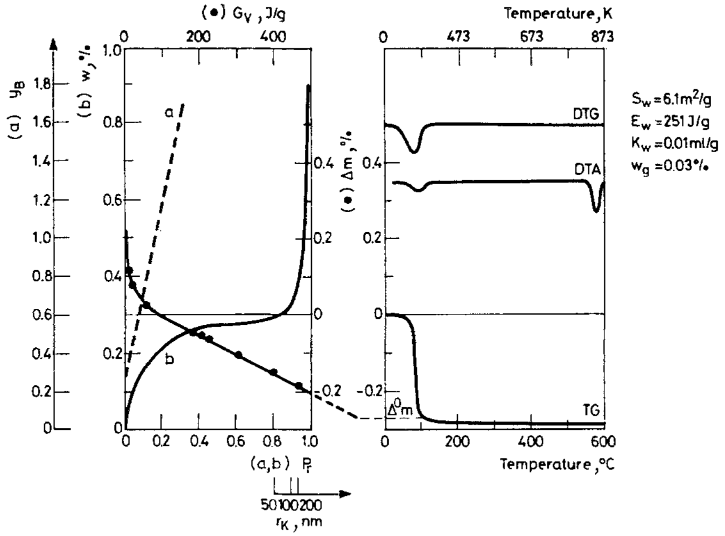

Fig. 3. Isotherms and thermal curves of quartz powder

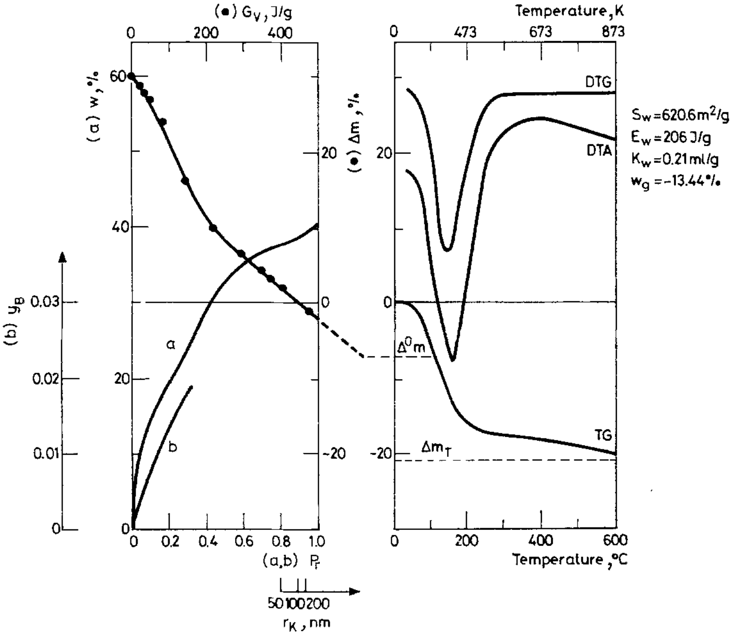

Fig. 4. Isotherms and thermal curves of silica gel

of the silica gel, mainly for the fine pore system and the larger external OH concentration, is higher than that of the quartz powder.

The difference between the peak temperatures of the thermoanalytical curves is mainly due to the differences between the surface polarities and the fine pore structures of the two materials.

Water vapour equilibria of montmorrillonites

Montmorrillonites (as adsorbents) have two important features: the large internal surface of the particles and the special surface structure containing different adsorption centres.

The large interval surface stems from the geometry of the crystal structure; the crystal is built up of triple layers that are arranged in parallel (as a card pack) in a very fine crystal. Water can diffuse between the layers, where it is adsorbed or condensed. The specific surface is very large (about 850 m^2/g) and about 80% of this is due to the internal surfaces of the layers [27, 28].

Formation of adsorption centres with different activities is due to the electric charge distribution of the crystal structure. The negative charge excess of the silicate skeleton is neutralized by exchangeable cations; thus, on the surface there are centres with both positive and negative charges.

Experiment. From natural Ca-bentonite containing 73% montmorrillonite, monocationic samples were prepared with lithium, sodium and potassium carbonate solutions, and examinations were made with combined method.

Experimental results (Figs 5 and 6)

The DTG curves of Ca and artificial Li-montmorillonite contain a double maximum indicative of adsorption centres with two different activities (Fig. 5, curves g, and h). Adsorption on the two active centres can be well followed (a–d) via the DTG curves. In the cases of K and Na-montmorillonite, double peaks can not be found at any water content (curves e, f), so it is possible that the activities of the two adsorption centres are approximately the same.

The specific surfaces, adsorption energies and capillarities calculated from the adsorption isotherms of the different specimens differ considerably from one another (Table 1).

Table 1

Specific adsorption values of monocationic bentonites

	Li-bentonite	Na-bentonite	K-bentonite
$S_w(m^2/g)$	318	546	222
E_w (J/g H_2O)	78	121	94
K_w (ml/g)	0.69	0.48	0.39

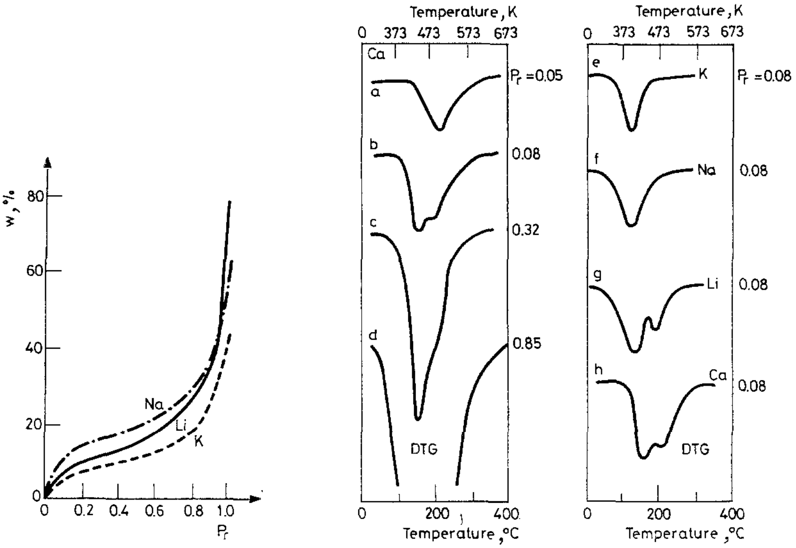

Fig. 5. Isotherms and DTG curves of bentonites (montmorillonites) prepared at different relative water vapour pressures

These experimental results, which are in contrast with principles such as the rule of the lyotropic series of the ions, can be well interpreted in terms of the further thermal analysis. If specimens are dehydrated, at 200° for several hours and then rehydrated, the DTG curves in Fig. 6 result for the pre-treated samples; after the treatment the K mineral shows no change; the peak temperature of the desorption of the Na mineral is decreased only slightly; while the second peak of the Li-montmorillonite disappears. The three cations display three disparate effects. The K^+ ions, connecting the triple layers, induce the irreversible decrease of the specific surface and the pore volume even during formation of the specimen; the Na^+ ions cause desaggregation of the mineral; the Li^+ ions, however, can enter the silicate skeleton, especially after removal of the water cover. A part of the triple layers of the heated Li-montmorillonite is blocked as regards the adsorption of water molecules (the specific surface decreases).

Bonding of water from the vapour phase by $CaSO_4$

Gypsum deprived of its crystal water by careful heating (anhydrite, $CaSO_4$-III) can bind water again even from the vapour phase. This latter process was studied by our combined method [29].

Experiment. Gypsum was transformed to anhydrite ($CaSO_4$-III) by heat treatment at 126° and then the adsorption isotherm (vapour pressure curve) was plotted. Equilibrium was attained within about 150 days. In the course of the attainment of

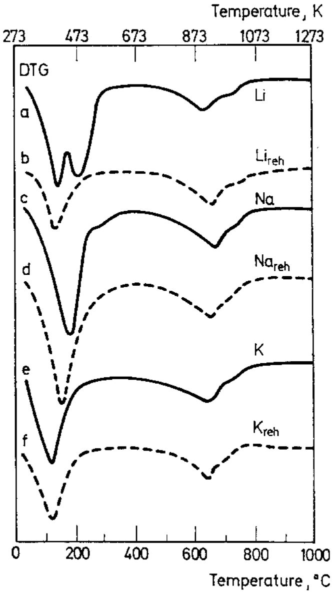

Fig. 6. DTG curves of monocationic bentonites in their original state and after heat treatment + rehydration ("reh")

equilibrium, samples were periodically taken from the anhydrite stored in saturated air and their TG and DTG curves were recorded (Fig. 7, DTG curves f–h).

Experimental results (Fig. 7)

From the adsorption isotherm calculation with the BET equation leads to a monomolecular adsorption saturation of $w_m = 6.76\%$; this would mean an unusually high (240 m^2g^{-1}) specific surface. Supposing that this water is bound by chemisorption, this quantity would correspond to 0.512 mol H_2O/mol $CaSO_4$. This supposion would also be justified by the high specific adsorption energy, but in itself this is not sufficient evidence.

From the thermal curves a and b, however, the formation of $CaSO_4 \cdot 0.5\ H_2O$ (hemihydrate) can be clearly established. Hence the adsorption equation is not applicable to the isotherm, for the value of the specific surface calculated is false and misleading.

The curves c–e clearly denote the formation of the dihydrate ($CaSO_4 \cdot 2\ H_2O$) on the capillary condensation line (thus not simple capillary condensation takes place). Curves f–h reveal that, though capillary condensation occurs in the first step (a peak below 100° in curves), the pore water later disappears because it takes part in dihydrate formation.

Thus, the reaction

$$(CaSO_4\text{-III})_s + 0.5\,(H_2O)_g = (CaSO_4 \cdot 0.5\ H_2O)_s$$

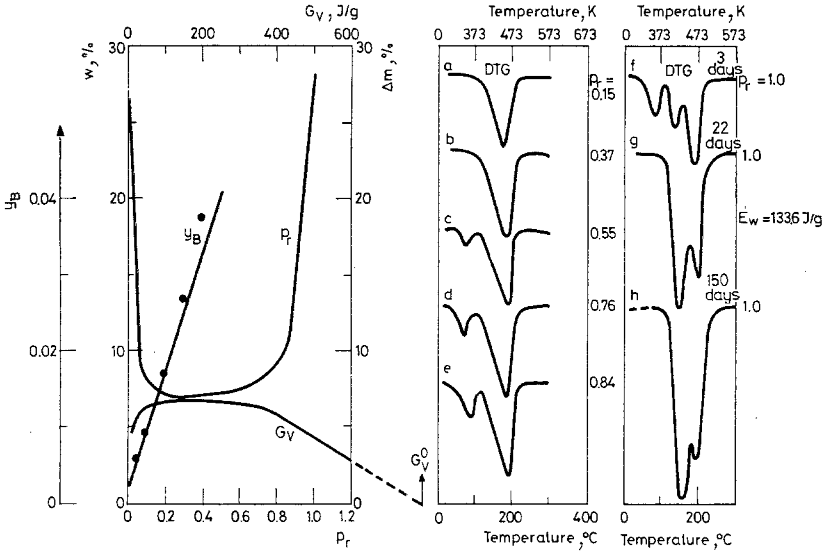

Fig. 7. Water vapour adsorption by $CaSO_4$-III.

can take place directly by the adsorption of water molecules as well. This is justified from a crystal chemical aspect, as it is known [34] that the crystal structures of $CaSO_4$ and the hemihydrate are identical. Accordingly, hemihydrate formation does not demand activity energy to be devoted to a change in crystal structure.

On the other hand, reactions such as

$$(CaSO_4 \cdot 0.5\,H_2O)_s + 1.5\,(H_2O)_f = (CaSO_4 \cdot 2\,H_2O)_s$$

$$(CaSO_4\text{-III})_s + 2\,(H_2O)_f = (CaSO_4 \cdot 2\,H_2O)_s$$

can occur only in the presence of condensed water. The process is actually a recrystallization with a change in the crystal structure: the $CaSO_4$ dissolves in the condensed water, the solution becomes oversaturated in the dihydrate, and the latter crystallizes out.

Water vapour adsorption by cement

The hydraulic hardening of cement is caused by hydration of the clinker minerals. Cement hydration can occur by water vapour adsorption, too [30, 31].

Experiment. The water vapour adsorption by cement was tested for 28 days. On the last day, thermoanalytical curves and desorption isotherms of samples with various water contents were determined.

Experimental results (Fig. 8)

It was established that no hydration occurs on the left (adsorption) line of the isotherms, so the water adsorption isotherms are suitable for determination of the specific surface of cements.

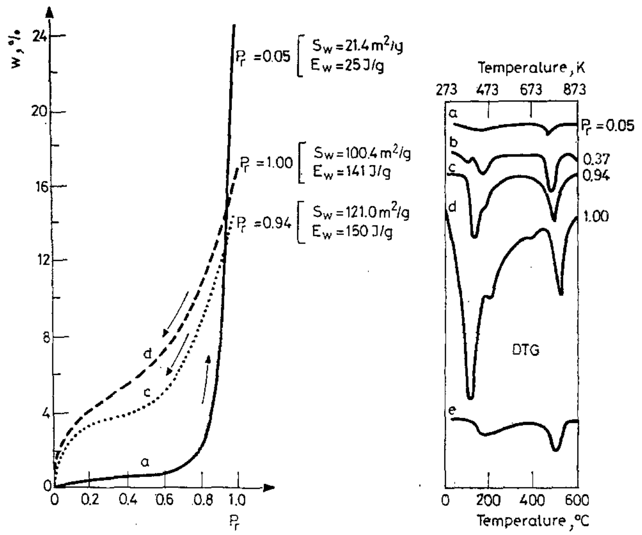

Fig. 8. Isotherms and DTG curves of cement *a—d)* Vapour pressure (adsorption (a) and desorption (c, d)) and DTG curves of cement stored for 28 days in air of different humidities; *e)* Cement stored for 28 days in saturated air, then for 150 days above concentrated sulphuric acid. The first peak practically disappeared from the DTG curve (the water binding is reversible)

Hydration processes can be found on the capillary condensation line of the isotherms, evidently due to the water condensed in the capillaries. At high humidity, hydration effects result in a decrease in the specific surface. This phenomenon can be explained by the coalescence of the particles. The water adsorption by cement hydrated for 28 days is reversible; water bound merely by chemical forces ($Ca(OH)_2$) can not be eliminated by desorption.

References

1. S. Gál, Die Methodik der Wasserdampf-Sorptionsmessungen, Springer-Verlag, Berlin, 1967.
2. R. C. Mackenzie, Differential Thermal Analysis, Vol. 1., 2. Acad. Press., London, 1969.
3. Derivatograph, Syst. E. Paulik, J. Paulik, L. Erdey MOM Budapest.
4. I. Barshad, Am. Mineral, 33 (1948) 655.
5. S. B. Hendricks, R. A. Nelson and T. Alexander, J. Am. Chem. Soc., 62 (1940) 1457.
6. I. Carnet, J. Chem. Phys., 18 (1950) 5.
7. T. Takamara, H. Hoshida and K. Inazuka, Koll. Z. 195 (1964) 12.
8. L. Imre, Építőanyag, 9 (1965) 353.
9. A. Páll, Építőanyag, 80 (1965) 353.
10. T. W. Parker, Clay Minerals, 8 (1969) 143.
11. R. Prost and J. Chanssidon, Clay Minerals, 25 (1973) 106.
12. K. Jónás, Építőanyag, 25 (1973) 106.
13. G. Englert, F. Wittmann and M. Nussbaum, Zement-Kalk-Gips, 4 (1971) 165.

14. V. V. MORAVIN and R. MILLS, J. Coll. Sci., 39 (1972) 406.
15. P. G. NUTTING, Adsorbent Clays, New York, 1943.
16. J. M. VLEESKENS, De rol van OH-groepen in silica, S-Gravenhage, Kitgeverij Excelsion, 1957.
17. S. BRUNAUER, L. S. DEMING, W. S. DEMING and E. TELLER, J. Am. Chem. Soc., 62 (1940) 1723.
18. Z. JUHÁSZ, Vízgőzadszorpció szilikátfelületen. (Adsorption of water vapour on silicate surfaces) Bp. Műsz. Egyetem. Építőanyagok Tanszék Tud. Közl. 30. KÖZDOK. Budapest, 1979.
19. S. BRUNAUER, P. H. EMMETT and E. TELLER, J. Am. Chem. Soc., 60 (1938) 309.
20. S. I. GREGG, Oberflächenchemie fester Stoffe, Verlag Technik, Berlin, 1958.
21. M. POLÁNYI, Z. angew. Chem., 35 (1922) 237.
22. M. M. DUBINYIN, Dokl. Akad. Nauk SSSR, 1947—1949.
23. G. VAN OLPHEN, J. Coll. Sci., 20 (1965) 822.
24. S. BRUNAUER and S. A. GREENBERG, Proc. IV. Int. Symp. on Chem. of Cement, Washington, 1960.
25. Z. JUHÁSZ, Aufbereitungs-Technik, 10 (1974) 559.
26. R. ZSIGMONDY, Kolloidchemie. Vlg. Springer, Leipzig, 1912.
27. R. W. MOONEY, A. G. KEENAN and L. A. WOOD, J. Am. Chem. Soc. 74 (1952) 1373.
28. R. E. GRIM, Clay Mineralogy, Mc Graw-Hill, London, 1953.
29. J. BOROS and Z. JUHÁSZ, Zement-Kalk-Gips, 5 (1973) 267.
30. T. C. POWERS and T. L. BROWNYARD, Studies of the physical properties of hardened p. cement paste. J. of the Am. Concrete Inst., Detroit, 1947.
31. Z. JUHÁSZ, Per. Polytechn., 17 (1973) 211.

ZUSAMMENFASSUNG — Prozesse und Gleichgewichte der Wasserdampfadsorption an Adsorbenten mit polarer Oberfläche können gut mit einer mit thermischer Analyse kombinierten Adsorptionsmethode getestet werden. Der erste Schritt der Methode schließt den Vergleich der Desorptions-Adsorptionsisothermen und der thermischen Kurven in sich ein, im zweiten werden Gleichgewichtspunkte der Adsorptionsisothermen durch thermische Analyse getestet.

Am Beispiel von einigen Baumaterialien werden die Möglichkeiten dieser Methode demonstriert. Die Adsorptionsisothermen waren formell in allen Fällen vom gleichen Typ und nur die vorgestellte komplexe Methode ergab, daß die Ausbildung des Gleichgewichtes durch grundsätzlich verschiedene Prozesse erfolgt. Solche Prozesse sind: von der Struktur des Adsorbenten und der Aktivität der aktiven Oberflächenzentren abhängige physikalische Adsorption Chemisorption, chemische Reaktion im Festkörper/Dampf-System und in der in Kapillaren kondensierten wässrigen Phase.

Резюме — Процессы адсорбции паров воды и равновесия адсорбентов с активными поверхностями могут быть испытаны каким-либо адсорбционным методом, совмещенным с термическим анализом. Первый шаг в этом методе включает сравнение изотермических кривых десорбция — адсорбция и термических кривых. Второй шаг — проверка изотермическим анализом различных равновесных точек адсорбционных изотерм. Возможности представленного метода показаны на примерах строителных материалов. Типы адсорбционных изотерм всех исследованных образцов были практически одинаковыми и только представленный комплексный метод дал возможность показать, что образование равновесий было вызвано различными процессами. Такими процессами являются: физическая адсорбция, зависящая от структуры адсорбента и активности внешних активных центров, хемисорбция, химическая реакция в системе твердое тело — газ и в водной фазе, сконденсированной в капиллярах.